FULLY-INTEGRATED CARBON NANOTUBE EPOXY FILM SENSORS FOR STRAIN SENSING IN GFRP

Christina Buggisch[a], Nils Felmet[a], Dennis Gibhardt[a], Bodo Fiedler[a]

a: Institute of Polymers and Composites, Hamburg University of Technology, Denickestraße 15, 21073 Hamburg, Germany
christina.buggisch@tuhh.de

Abstract: *Structural health monitoring of fiber-reinforced polymer composites becomes more important to ensure a safe and reliable operation. This work demonstrates a method for local matrix modification of glass fiber-reinforced polymers with fully-integrated pre-cured carbon nanotube epoxy thin-film sensors enabling a piezo-resistive strain and damage monitoring. The film sensors were manufactured using a manual film applicator, partially pre-cured for 48 h under lab conditions, cut to shape, and placed on dry glass fiber fabrics before infusion in a resin transfer molding process. Three-point bending tests with sensor films under the upper ply, in the middle, and over the lower ply prove the sensor films' ability for localized strain monitoring. Furthermore, detection of critical buckling is possible in structural parts, as demonstrated in compression tests of coupon specimens and stringer components.*

Keywords: Structural Health Monitoring; Damage Detection; Multifunctional Composite

1. Introduction

Fiber-reinforced polymer composites exhibit a complex failure behavior due to their multi-scale nature. In-situ damage monitoring during operation, referred to as structural health monitoring (SHM), can significantly enhance safety and reliability. Many advanced SHM methods, e.g., fiber Bragg sensors, electrical measurements, acoustic emission, and wave propagation, have been developed and are part of ongoing research [1]. Most of these methods require skilled personnel or expensive measuring equipment. Therefore, standard surface-mounted strain gauges are still widely used for strain and damage monitoring of composite structures. However, surface-mounted strain gauges are susceptible to external influences, merely monitor small areas, and cannot monitor internal strains.

The intrinsic electrical conductivity of carbon fibers enables self-sensing of strain and damage detection in carbon fiber-reinforced polymers with electrical resistance measurements [2, 3]. Due to a lack of material conductivity, unmodified glass fiber-reinforced polymers (GFRP) do not exhibit such self-sensing behavior. However, a modification of the polymer matrix with conductive nanoparticles such as carbon nanotubes (CNTs) can enable electrical conductivity when the filler content is above the percolation threshold. Load application leads to a resistance change due to a change of the conductive CNT network paths known as piezo-resistive effect. The piezo-resistive strain-sensing ability of GFRPS with a fully nanoparticle-modified polymer matrix was studied by many researchers for different load cases [4, 5].

However, fully modifying the polymer matrix is expensive and does not allow localized damage monitoring. Surface-mounted CNT/polymer sensors have demonstrated promising results on various substrates but experience similar limitations as classic metal strain gauges [6]. Furthermore, different methods for localized integration of CNTs have been proposed, like

  doi:10.5075/epfl-298799_978-2-9701614-0-0

dipping selected dry glass fabrics in aqueous CNT dispersions [7], spray-coating CNTs on dry glass fiber fabrics [8], integrating aligned CNT sheets [9] or buckypapers [10], and applying CNTs using frictional roller sliding [11].
Within this work, fully-integrated pre-cured CNT/epoxy thin-film sensors for piezo-resistive strain and damage monitoring are demonstrated. The flexible film sensors can easily be cut to the desired shapes and integrated in standard industrial infusion processes. Therefore, the proposed method enables a tailored SHM via electrical resistance measurements.

2. Materials and Methods

2.1 Manufacturing of Sensor Films

A homogeneous paste containing the amine-based two-component epoxy system EPIKOTE™ Resin MGS™ RIMR 135 and EPIKURE™ Curing Agent MGS™ RIMH 137 (Hexion Inc., USA) and 0.5 wt.% OCSiAl Tuball™ SWCNT was manufactured using a three-roll mill process further described in [12, 13]. The film sensors with a thickness of 6 mils (152.4 µm) were applied on a polished steel plate covered in Polytetrafluoroethylene (PTFE) foil using a manual film applicator BYK 5358 (BYK-Gardner GmbH, Germany) and partially pre-cured for 48 h under lab conditions.

2.2 Manufacturing of Laminates

The pre-cured films were cut to the desired shapes, removed from the PTFE foil, and placed on dry non-crimp E-glass fiber fabrics UT-E250 and UT-E500 (Gurit Holding AG, Switzerland) before infusion in a vacuum-assisted resin transfer molding process using a closed aluminum mold. The two-component epoxy system used for film manufacturing was also used as infusion resin to achieve a sufficient chemical bonding between the integrated films and the surrounding polymer matrix. The unidirectional (UD) laminates were cured in a heat press at 50 °C for 16 h and post-cured in an oven at 80 °C for 16 h.

2.2 Manufacturing of Coupon Specimens

The specimens were cut to the dimensions specified in Table 1 using an ATM Brillant 265 precision saw (ATM Qness GmbH, Germany). The compression specimens were equipped with 1 mm-thick GFRP loading tabs before cutting. Therefore, the gripping areas and loading tabs were ground using 600 grit sanding paper and cleaned with isopropanol. The two-component epoxy paste adhesive UHU Endfest 300 (UHU GmbH & Co. KG, Germany) was used to bond the loading tabs to the specimens. The adhesive was cured for 60 min at 60 °C using a heat press. For electrical contacting, LiFy copper cables with a cross-section of 0.25 mm² were attached to the specimen edges using Acheson 1415 conductive silver paint (PLANO GmbH, Germany). Figure 1 shows the specimen configurations, including sensor film and contacting positions.

Table 1: Lay-up and film positions of unidirectional coupon specimens.

Specimen type	Size	Film Position
Bending	100x15x2 mm³	Under top ply, Middle, Above bottom ply
Compression	130x10x4 mm³	Middle

  doi:10.5075/epfl-298799_978-2-9701614-0-0

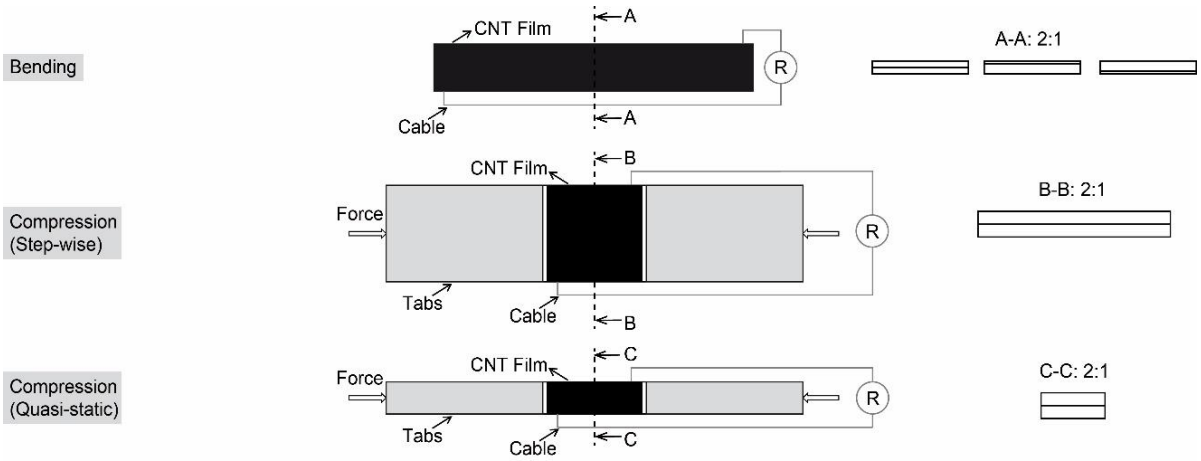

Figure 1. Schematics of coupon specimens including film and contacting positions

2.3 Manufacturing of Stringers

Stringers were manufactured in a vacuum-assisted infusion process on an open aluminum mold using a vacuum bag setup. The stringers had a $[\pm 45/0_3]_s$ lay-up consisting of bidiagonal ±45° glass fiber fabrics B320E-H (HP-Textiles GmbH, Germany) and UD UT-E250 (Gurit Holding AG, Switzerland) non-crimp glass fiber fabrics. The film sensors were integrated under the top ±45°-layer. The infusion resin was the same two-component epoxy system also used for film and laminate production. Curing was performed at room temperature for 48 h and post-curing took place in an oven at 80 °C for 16 h. The backing plate was manufactured as described in Section 2.2 using UT-E250 (Gurit Holding AG, Switzerland) fabrics and a $[0_2/90/0_2]_s$ lay-up. Stringer and backing plate were cut to a size of 245 x 127 mm² and adhesively bonded using the two-component epoxy paste adhesive UHU Endfest 300 (UHU GmbH & Co. KG, Germany) following the process described in Section 2.2. Curing of the adhesive was performed for 1 h at 60 °C in an oven. Afterward, both stringer ends were cast 30 mm deep in epoxy resin as load introduction elements. Furthermore, the backing plate was spray-painted with a random speckle pattern for digital image (DIC) correlation measurements. The electrical contacting was carried out in the same way as for the coupon samples. The positions of the film sensors and the electrical contacting are shown in Figure 4.

2.4 Test Setup

Force-controlled step-wise and quasi-static tests until final failure were conducted for three-point bending (TPB) and compression coupon tests. The TPB tests were performed on a Z10 universal testing machine (ZwickRoell GmbH & Co. KG, Germany) according to DIN EN ISO 14125 [14]. The support distance was 60 mm, the upper roller diameter 15 mm, and the lower roller diameters were chosen as 10 mm. The test speed was 2 mm min^{-1}. Compression tests on coupon specimens and the crippling test on the stringer were conducted on a Z400 universal testing machine (ZwickRoell GmbH & Co. KG, Germany). Compression tests were performed in shear mode following ASTM D3410 [15] using a hydraulic combined loading fixture. Crippling tests of the stringers were performed with a constant speed of 0.25 mm min^{-1}. An ARAMIS 4M DIC system was used to monitor the deformations and buckling of the stringers. The in-situ electrical resistance was measured during all tests using a Keithley 2601A (one film sensor – coupon specimens) or a Keithley 2602 (two film sensors – stringers). Therefore, a constant voltage of 1 V was applied and the current was measured.

  doi:10.5075/epfl-298799_978-2-9701614-0-0

3. Results and Discussion

3.1 Three-Point Bending Tests

Figure 2 shows representative results of step-wise TPB tests on UD specimens with CNT sensor films under the upper ply, in the middle of the laminate, and over the lower ply, including stress and resistance changes over time. The resistance change ΔR in % is calculated according to Equation (1)

$$\Delta R = \frac{R-R_0}{R_0} 100\,, \tag{1}$$

with initial resistance R_0 and current resistance R. In general, all three configurations show a different resistance change behavior. The resistance changes result from the piezo-resistive behavior of the CNT epoxy film sensors and the variation of the CNT network as a consequence of the loading.

Due to their placement above the neutral axis, the sensor films under the upper ply experience compressive stress resulting in an anti-proportional and negative resistance change which is fully reversible for small loads and increasingly irreversible with higher loads. The compressive strain leads to a formation of new conductive paths or a reduction of the tunneling resistance as CNTs are moved closer together [16, 17]. The irreversibility is caused by irreversible network changes inside the CNT film sensors, e.g., due to the indentation at the rollers.

Film sensors integrated in the middle of the laminate show a small and mixed positive and negative resistance change. As in theory only shear and no volume change is expected in the neutral axis during bending, the influence of the loading on the CNT network and the resistance change should be minimal for film sensors in the middle of the laminate. The measured resistance change is significantly smaller than in film sensors under the upper or above the lower ply. The small and mixed positive and negative resistance changes can be explained by deviations of the films with respect to the neutral axis due to, e.g., the films' thickness and manufacturing-related waviness.

Placing the film sensors over the lowest ply induces tensile stresses in the film that result in a positive resistance change proportional to the applied stress. Conductive paths inside the film sensors dissolve under tensile load as CNTs are pulled further apart or lose contact. The resistance change is fully reversible during the first three load steps. Afterward, the resistance drops below the initial resistance when fully unloading the samples, indicating more conductive paths or closer CNTs inside the sensors.

TPB tests generally reveal the sensor film's ability to detect local stresses inside the GFRP and monitor the applied stresses. Due to the piezo-resistive effect, monitoring the stress or strain inside the material is possible by measuring the resistance change. A threshold value of the resistance change can be specified to ensure a safe and reliable operation of the respective GFRP part. A more detailed analysis, including the sensor films' influence on the mechanical properties and the sensing results of bending and tensile tests of UD and cross-ply specimens, can be found in [13].

  doi:10.5075/epfl-298799_978-2-9701614-0-0

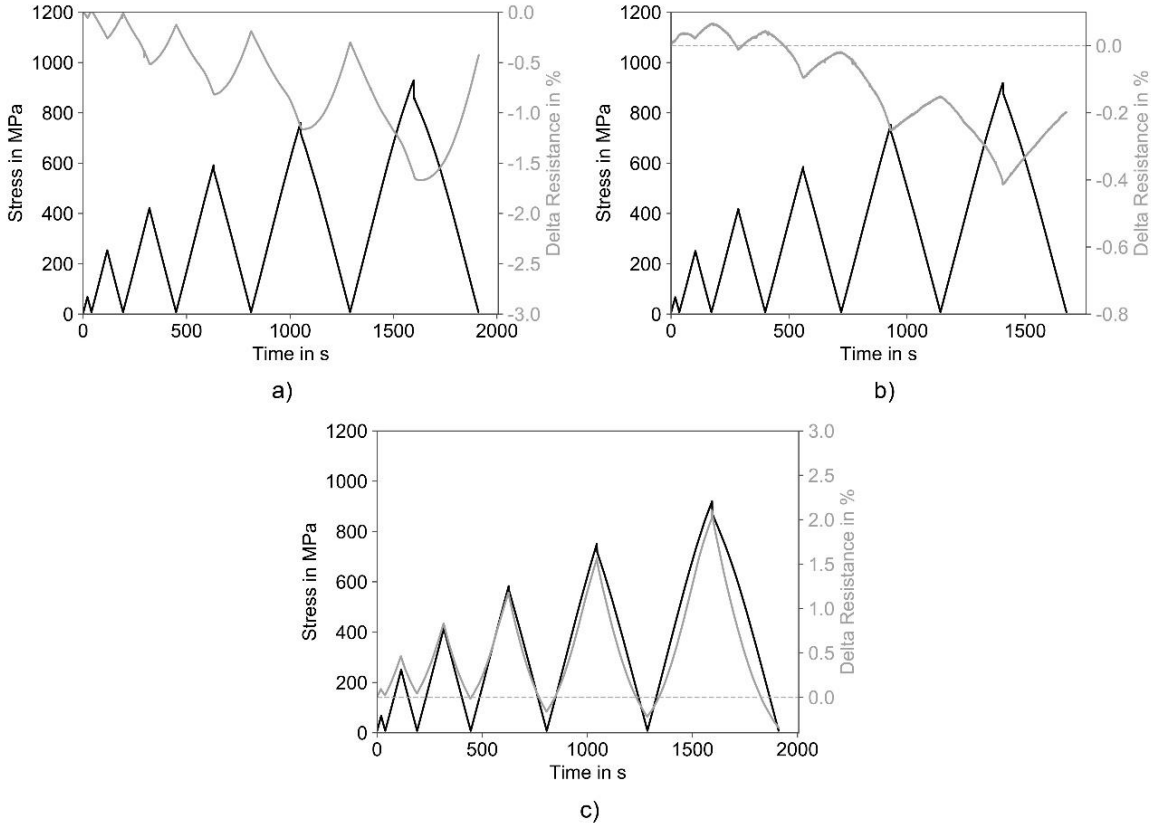

Figure 2. Representative results of quasi-static bending tests on UD specimens - a) Sensor film under the upper ply, b) Sensor film in the middle, c) Sensor film over the lower ply

3.2 Compression Tests

Representative results of step-wise and quasi-static compression tests until failure on UD coupon specimens are shown in Figure 3.

Following the findings of the bending tests and the piezo-resistive behavior, a stress anti-proportional resistance change is expected during compression tests. The step-wise tests (compare Figure 3 a)) show the expected anti-proportional agreement of the resistance change with the applied stress and a fully reversible resistance change during unloading, which implies no irreversible changes in the CNT network due to damages. No buckling or damaging of the specimens was observed in the step-wise tests.

To ensure failure in the shear loading setup, the specimens loaded until final failure were less wide (compare Table 1) and experienced visible buckling. As visible in the representative results in Figure 3 b), the measured resistance change is anti-proportional with the applied stress in the beginning but starts to increase after approximately 10 s. This increasing resistance change correlates with a slight slope change in the stress-time curve and with visible buckling of the specimens during the tests. As a result of the buckling, the sensor films no longer encounter a pure compressive load. Instead, the buckling introduces a bending of the integrated sensor films, which explains the resistance increase.

Consequently, buckling during compression tests can reliably be detected by an unexpected resistance increase without an associated load decrease.

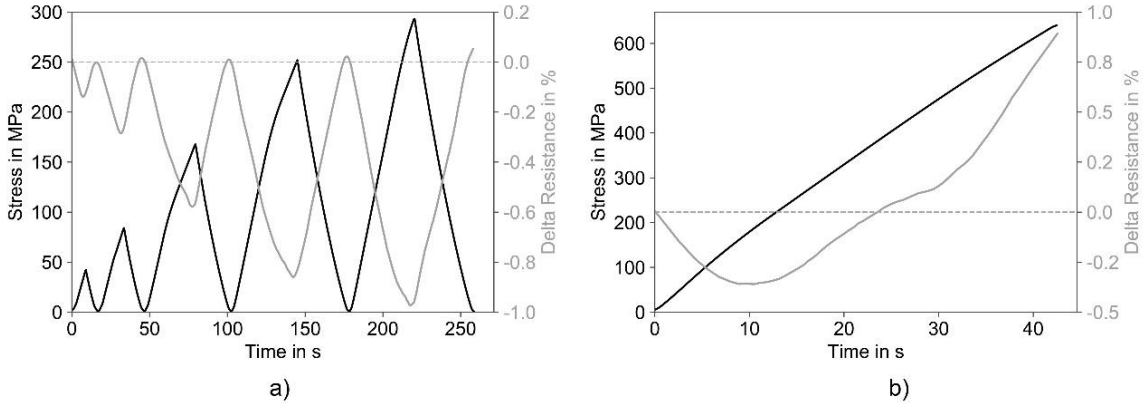

Figure 3. Representative results of quasi-static compression tests on UD specimens - a) Step-wise test, b) Until final failure.

3.3 Crippling Tests

Crippling tests on stringers were conducted to evaluate the sensor films' behavior in larger components. The results of a representative compression test on a stringer are shown in Figure 4, including force, resistance change, and corresponding DIC images. The DIC images show the z-displacement of the backing plate of the stringer.

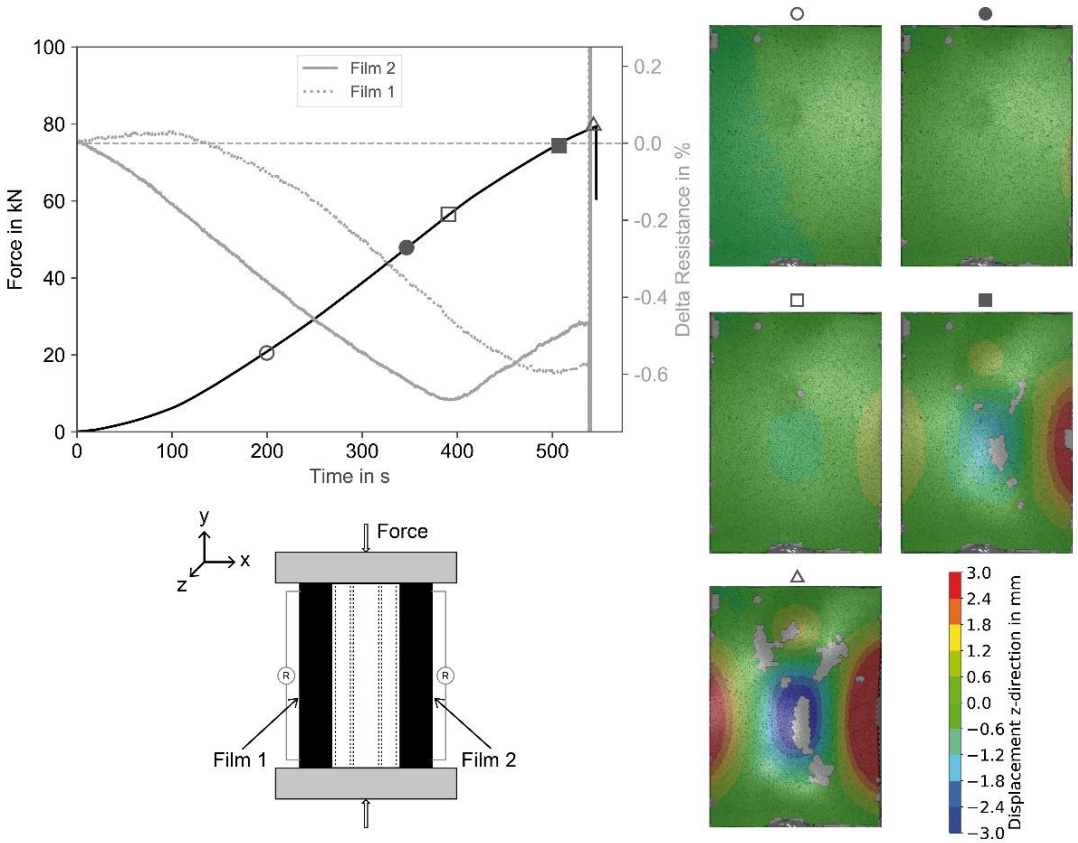

Figure 4. Results of crippling test on stringer component with two fully-integrated CNT/epoxy film sensors including force, resistance change, and digital image correlation images with displacement in z-direction.

At the beginning of the test, film sensor 2 shows a resistance change that is anti-proportional with the applied load and the DIC images reveal no buckling. From 400 s onwards, the resistance change starts to increase. At this time, the according DIC image reveals a significant z-displacement in the area of film 2 visible as a yellow area. The stringer starts to buckle. Until final failure, the buckling becomes more and more severe as visible by the growing z-displacement and the resistance change is increasing further.

The resistance change measured in film sensor 1 shows delayed behavior. Up to approximately 150 s, almost no resistance change is visible. After that, the resistance starts to decrease with a similar slope as observed for film sensor 2. The whole remaining course of the resistance change, including the resistance increase in film sensor 1, is measured with a time delay. The DIC images also reveal a delayed buckling in the area of film sensor 1. While no z-displacement is visible in the area of film sensor 1 at 400 s, film sensor 2 already displays a significant z-displacement. The time shift can be explained by a non-uniform load introduction.

The results prove the sensor films' ability to detect undesired critical buckling during compressive loading in coupon specimens and bigger components like the presented stringer.

4. Conclusion

The presented fully-integrated pre-cured CNT epoxy film sensors allow for piezo-resistive strain and damage monitoring of GFRPs. A reproducible piezo-resistive correlation between strain and resistance change is possible. Tensile stresses result in a strain-proportional resistance increase and compressive stresses in a resistance decrease which is anti-proportional to the applied stress.
Integration in different layers in TPB tests showed the potential for localized strain state evaluation inside the material.
Furthermore, the results of compression tests on coupon samples and crippling tests on stringers proved the reliable detection of critical buckling by a resistance increase during compressive loading.
In general, the thin-film sensors allow for tailored strain and damage monitoring of GFRP by offering large design freedom, including measurements at different material depths, over large sections, or in highly loaded areas. The flexible, pre-cured sensor films can easily be handled, cut to the desired shapes, placed on dry glass fiber fabrics, and thus be used in standard (industrial) vacuum infusion processes. Furthermore, the introduction of these fully integrated thin-film sensors does not lead to any strength reduction.

Acknowledgments
This research was funded by the German Research Foundation (DFG) within the project number 393868053.

5. References

1. Diamanti K, Soutis C. Structural health monitoring techniques for aircraft composite structures. Progress in Aerospace Sciences. 2010; 46:342–352. doi: 10.1016/j.paerosci.2010.05.001.
2. Schulte K, Baron C. Load and failure analyses of CFRP laminates by means of electrical resistivity measurements. Composites Science and Technology. 1989; 36:63–76. doi: 10.1016/0266-3538(89)90016-X.

3. Abry JC, Choi YK, Chateauminois A, Dalloz B, Giraud G, Salvia M. In-situ monitoring of damage in CFRP laminates by means of AC and DC measurements. Composites Science and Technology. 2001; 61:855–864. doi: 10.1016/S0266-3538(00)00181-0.
4. Thostenson ET, Chou T-W. Carbon Nanotube Networks: Sensing of Distributed Strain and Damage for Life Prediction and Self Healing. Adv. Mater. 2006; 18:2837–2841. doi: 10.1002/adma.200600977.
5. Böger L, Wichmann MHG, Meyer LO, Schulte K. Load and health monitoring in glass fibre reinforced composites with an electrically conductive nanocomposite epoxy matrix. Composites Science and Technology. 2008; 68:1886–1894. doi: 10.1016/j.compscitech.2008.01.001.
6. Kang I, Schulz MJ, Kim JH, Shanov V, Shi D. A carbon nanotube strain sensor for structural health monitoring. Smart Materials and Structures. 2006; 15:737–748. doi: 10.1088/0964-1726/15/3/009.
7. Gao S-L, Zhuang R-C, Zhang J, Liu J-W, Mäder E. Glass Fibers with Carbon Nanotube Networks as Multifunctional Sensors. Adv. Funct. Mater. 2010; 20:1885–1893. doi: 10.1002/adfm.201000283.
8. Rodríguez-González JA, Rubio-González C, Soto-Cajiga JA. Piezoresistive Response of Spray-coated Multiwalled Carbon Nanotube/Glass Fiber/Epoxy Composites under Flexural Loading. Fibers Polym. 2019; 20:1673–1683. doi: 10.1007/s12221-019-8711-8.
9. Aly K, Li A, Bradford PD. Strain sensing in composites using aligned carbon nanotube sheets embedded in the interlaminar region. Composites Part A: Applied Science and Manufacturing. 2016; 90:536–548. doi: 10.1016/j.compositesa.2016.08.003.
10. Slobodian P, Lloret Pertegás S, Riha P, Matyas J, Olejnik R, Schledjewski R, Kovar M. Glass fiber/epoxy composites with integrated layer of carbon nanotubes for deformation detection. Composites Science and Technology. 2018; 156:61–69. doi: 10.1016/j.compscitech.2017.12.012.
11. Kravchenko OG, Pedrazzoli D, Bonab VS, Manas-Zloczower I. Conductive interlaminar interfaces for structural health monitoring in composite laminates under fatigue loading. Materials & Design. 2018; 160:1217–1225. doi: 10.1016/j.matdes.2018.10.045.
12. Meeuw H, Wisniewski VK, Köpke U, Nia AS, Vázquez AR, Lohe MR, Feng X, Fiedler B. In-line monitoring of carbon nanoparticle epoxy dispersion processes. Prod. Eng. Res. Devel. 2019; 13:373–390. doi: 10.1007/s11740-019-00884-5.
13. Buggisch C, Gibhardt D, Felmet N, Tetzner Y, Fiedler B. Strain sensing in GFRP via fully integrated carbon nanotube epoxy film sensors. Composites Part C: Open Access. 2021; 6:100191. doi: 10.1016/j.jcomc.2021.100191.
14. DIN EN ISO 14125. Fibre-reinforced plastic composites - Determination of flexural properties; 2011.
15. ASTM D3410. Standard Test Method for Compressive Properties of Polymer Matrix Composite Materials with Unsupported Gage Section by Shear Loading. West Conshohocken, PA: ASTM International.
16. Hu N, Karube Y, Yan C, Masuda Z, Fukunaga H. Tunneling effect in a polymer/carbon nanotube nanocomposite strain sensor. Acta Materialia. 2008; 56:2929–2936. doi: 10.1016/j.actamat.2008.02.030.
17. Wichmann MHG, Buschhorn ST, Gehrmann J, Schulte K. Piezoresistive response of epoxy composites with carbon nanoparticles under tensile load. Phys. Rev. B. 2009; 80:667. doi: 10.1103/PhysRevB.80.245437.

